A Mesoporous Pattern Created by Nature in Spicules from *Thetya aurantium* Sponge

Gianluca Croce,* Davide Viterbo,* Marco Milanesio,* and Heinz Amenitsch†
*DISTA, Università del Piemonte Orientale, Alessandria, Italy; and †Institute of Biophysics and Nanosystems Research (IBN), Austrian Academy of Sciences c/o Sincrotrone Trieste, Basovizza (TS), Italy

ABSTRACT Siliceous or carbonate spicules provide support and defense to marine sponges. The inorganic envelope usually embodies a protein core. Our SAXS study of the siliceous spicules from the demosponge *Thetya aurantium* proves the very ordered structure assumed by the protein core inside the spicules. Indeed, not only the very sharp diffraction spots already found in previous studies on spicules from different sponges are confirmed, but also the 11 sharp spots in the diffraction pattern recorded after thermal treatment at 250°C can only be interpreted in terms of a natural nanocomposite mesostructure with an hexagonal lattice formed by a three-dimensional periodic arrangement of silica cages in which the protein units act as structure directing agent.

INTRODUCTION

Sponges are primitive marine animals and consist of organized cells supported by a skeleton of inorganic fibers known as spicules. Spicules are usually composed of calcium carbonate or of silica, and their secretion is due to specialized cells called sclerocytes (1). The two most important functions of the spicules are to provide support for the soft part of the sponges and to play a defense role. Their inorganic envelope generally contains an organic proteic axial filament (2). Proteins from siliceous spicules are called silicateins (3) (for SILICA proTEINS) and the biological formation of amorphous hydrated silica, called biosilicification, probably occurs under the control of these specialized biomolecules (4). The organic matrix is thus suggested to play a critical role in the catalysis of silica polycondensation reactions and in the structure organization (5).

Spicules may show very different and complex shapes and the molecular mechanisms leading to their formation is still rather unclear. Some of them contain an organic axial filament around which hydrated silica is deposited. The concentric arrangement of the silica is the result of a periodic secretion. Siliceous spicules are formed at the intracellular level by the deposition of hydrated silica around the protein filament. This filament, although present immediately before silicification, continues to grow during silica deposition. It is generally assumed that spicule growth is a bidirectional process: the increase in length is affected by the elongation of the filament, whereas the increase in width is determined by the apposition of the silica.

In recent years, we have carried out an extensive structural study on a number of siliceous spicules from sponges belonging to different families (6,7) using a wide variety of experimental and theoretical approaches. The most important results of these studies on the structural organization of the silicatein filament inside the spicules are: i), the very high degree of periodic regularity indicated by the very sharp diffraction spots obtained by our diffraction experiments; ii), the different arrangement and packing of the protein units in spicules from sponges of two different phylogenetic classes: in the demosponge *Thetya aurantium* or *Geodia cydonium*, a fairly dense hexagonal packing of parallel tubular protein units separated by ~5.8 nm can be postulated, whereas in the hexactinellid *Scolymastra joubini*, a less dense hexagonal packing of spirally oriented cylindrical protein units separated by ~8.4 nm is consistent with our diffraction data (6).

In this study we have concentrated our attention on siliceous spicules extracted from *Tethya aurantium* sponges belonging to the demosponge family, because of their rich small angle x-ray diffraction pattern (6). These spicules have an elongated shape with one sharp and one rounded tip (strogyloxeas) (8) and a length of 2–2.5 mm and a section of 15–20 μm. In previous works, we revealed the presence of bioorganic matter in the central cavities inside the inorganic envelope by electron microscopy on grinded samples and by thermogravimetric measurements (6,7). These cavities are the sites where the silicatein proteins, responsible for the spicule growth, are hosted (9). Extraction of the bioorganic matter from the silica envelope can only be performed by a rather strong treatment with HF/NH_4F solutions, which may cause relevant structural changes. To obtain some structural information on the untreated organic filaments as they are inside the spicules and to achieve a more realistic and detailed picture of their organization, small angle x-ray diffraction measurements were carried out at the SAXS beamline of the ELETTRA synchrotron radiation facility.

MATERIALS AND METHODS

Megasclere spicules extracted from *T. aurantium* sponges, collected in the coastal lagoon of Porto Cesareo (Apulian Coast), are freed from the external

Submitted August 3, 2006, and accepted for publication September 8, 2006.

Address reprint requests to Gianluca Croce, E-mail: gianluca.croce@mfn.unipmn.it.

0006-3495/07/01/288/05 $2.00

doi: 10.1529/biophysj.106.094532

organic matter by immersion in hydrogen peroxide (200 vol) changed each day for two weeks. They are then rinsed in distilled water and dried at 60°C.

Diffraction experiments on these megascleres were carried out by the Austrian SAXS beamline (BL 5.2 L) (10) of the ELETTRA Synchrotron Light Laboratory (Trieste, Italy), using x-rays of wavelength $\lambda = 0.1540$ nm and SAXS data were collected with a two-dimensional charge-coupled device-detector (diameter 115 mm; Photonic Science, Robertsbridge, UK), positioned at 872.4 mm from the sample. For the *T. aurantium* spicules, the samples were still bundles of 10–15 almost parallel spicules inside a boron glass capillary, to increase the diffraction signals. Single spicules of *T. aurantium* were also mounted on a sample holder to perform single-fiber diffraction experiments while rotating the sample by 180°. High temperature measurements were carried out using tight bundles of parallel spicules to avoid possible disorientation of the sample caused by heating. For the in situ experiments a temperature gradient cell for x-ray scattering measurements was used. The samples were heated up to 250°C with a ramp of 1°C/min and the diffraction data were collected every 5°C after an isotherm of 5 min. The ex situ experiments were carried out heating different spicule bundles in a lab oven, where the samples were kept isothermally at 50°C, 100°C, 150°C, 200°C, and 250°C for 1 h and cooled for 30 min before the diffraction data collection. A bundle of spicules was also maintained at 250°C for 72 h and cooled for 24 h before the measurements.

In all experiments, the elongation axis of the spicule was along the horizontal *x* axis of the patterns. Therefore the spots along the central vertical line (*y* axis) are the equatorial spots, whereas the polar spots are along the horizontal *x* axis. The two-dimensional data were processed using the FIT2D program (11,12). Before the analysis of the SAXS data, the collected images were corrected with FIT2D for the following factors: normalization of the intensity, spatial distortion and subtraction of the instrumental errors (background noise and dark current).

RESULTS AND DISCUSSION

Diffraction patterns were collected from still samples composed by bundles of almost parallel spicules and from single spicules mounted on a rotating holder, as described in the Materials and Methods section. The *T. aurantium* bundles were also heated from room temperature to 250°C, to shed some light on the structural rearrangements accompanying the thermal decomposition of the organic material.

The diffraction pattern from a still bundle, collected at room temperature (Fig. 1 *a*) reveals three very sharp independent diffraction spots. The most intense spot is in the vertical (equatorial) position, whereas the other two are in nonequatorial positions. The former spot has an estimated value of d-spacing of ~5.0 nm typical of spicules belonging to the demosponge family (6,7). The most striking feature of our results is the appearance of ''single crystal like'' diffraction spots, which are much too sharp to be ascribed to the usually rather broad diffraction effects by fibers and indicate a high degree of structural order and periodicity. Indeed, the reciprocal space image of a bundle of parallel columns with a randomly oriented periodic lattice is a set of circles and the observed diffraction spots appear at the intersections of these circles with the Ewald sphere. The high degree of structural order is confirmed by the rotation patterns from a single spicule. Indeed the sequence of patterns recorded every 1° of rotation shows the same sharp spots and arrangement found in Fig. 1 *a*, revealing the presence of a three-dimensional structural order. From just these three independent spots it is impossible to derive a model of the structural organization inside *T. aurantium* spicules.

The surprising effects of the in situ thermal treatment on these three spots are an increase both in their intensity and in their sharpness, as well as a small shift of the maxima toward higher angles (decrease of the d-spacings). Besides at higher temperatures new spots emerge in the diffraction pattern and at 250°C (Fig. 1 *b*) eleven independent spots are observed.

Let us have a closer look at the relevant changes on the SAXS pattern caused by the thermal treatments on the *T. aurantium* spicules. The integration along the (10l) reciprocal lattice direction of the three spots common to all the patterns taken at different temperatures is shown in Fig. 2 *a*. These spots not only persist at all temperatures, but slightly increase in intensity and also show a small but significant change in position with a shift toward higher 2θ values at higher temperatures and in Table 1 the corresponding decrease in the d-spacings is reported. The radial integration along the (*00l*) polar axis of all the patterns is shown in Fig. 2 *b*, where the appearance at higher temperatures of three new peaks at $2\theta = 0.8°$, 1.6°, and 2.4° (d-spacings of 11.4, 5.6, and 3.7 nm) can be observed.

It is worth noting that the same effects on the diffraction spots were observed with all the ex situ experiments, indicating that the thermal treatment induces the formation of a more ordered phase. Nevertheless, after a 72 h isothermal treatment at 250°C no signal was recorded, indicating that the high temperature phase is destroyed after a prolonged heating (13).

In the diffraction pattern of *T. aurantium* taken at 250°C 11 sharp spots are present and their d-spacings are listed in the fourth column of Table 2. Their positions are consistent with a hexagonal lattice with approximate unit cell parameters

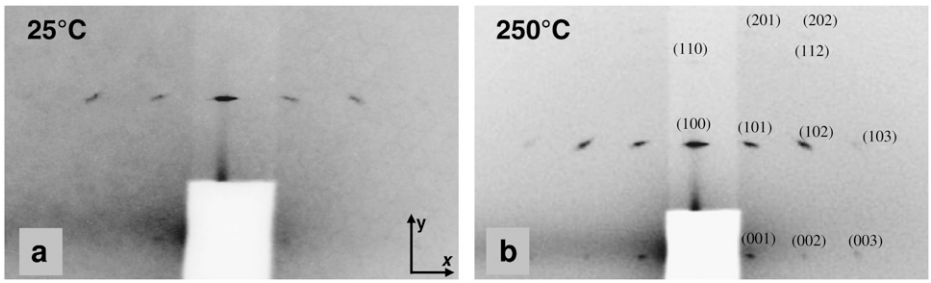

FIGURE 1 Diffraction patterns of a bundle of *T. aurantium* spicules. Patterns collected (*a*) at room temperature and (*b*) at 250°C are shown.

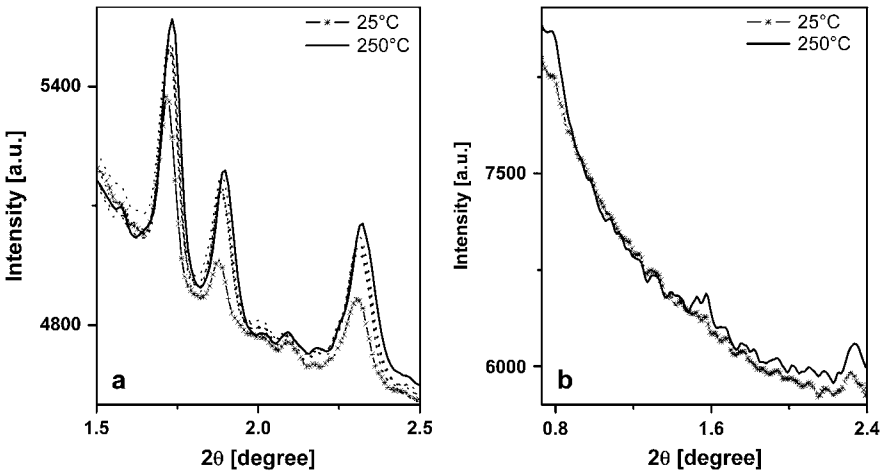

FIGURE 2 One-dimensional plots during heating from 25 to 250°C. The trend of (*a*) the one-dimensional linear integration along the (*10l*) reciprocal lattice and (*b*) of the spots along the (*00l*) polar axis, are shown.

$a = b = 5.9$ nm, $c = 11.4$ nm, in which all the 11 spots can be indexed as shown in the first three columns of Table 2. After a least-square refinement based on all reflexions, the cell parameters become $a = b = 5.8$ nm, $c = 11.2$ nm and the values of the calculated spacings d_{cal} and the differences $\Delta d = d_{cal} - d_{obs}$ are reported in the last two columns of Table 2.

These results confirm the high degree of periodic order in our samples and support the hypothesis of an arrangement of the protein units similar to that of the pores in highly ordered siliceous mesoporous materials (14–17), which indeed give sharp diffraction patterns similar to those we have obtained from spicules (6,7). The sharp diffraction spots and the unexpected behavior after thermal treatments indicate that the examined system is more complex than just a simple organic filament in the central hole of the megascleres. In this case the diffraction spots would not be so sharp and one would expect that at temperatures above 100°C the protein units would initiate an unfolding and/or decomposition process, yielding to a decrease of the degree of order, with a consequent decrease of intensity and sharpness of the diffraction spots. We have instead an opposite behavior and the disappearance of the diffraction effects is only achieved after ex situ prolonged thermal treatments. This is consistent with the findings that a significant amount of silica is also present in the central axial hole, where the organic matter is located, as already suggested by previous studies (18,19). Our structural model of a highly crystalline hexagonal arrangement of protein units, organized as a siliceous mesoporous nanostrucure within the spicule axial hole, shed some light also on the structural features observed by previous TEM studies (19,20).

The features of our diffraction patterns must only be indirectly related to the arrangement of the protein units, and strongly support our hypothesis that they are instead due to the presence of an ordered mesoporous siliceous system (21–24) inside the spicules, where the proteins act as templates. Indeed, the increased order observed at 250°C can actually be the consequence of two concurring effects: i), the unfolding and/or decomposition of the protein units inside the spicules causing and increase of the electron density contrast between the siliceous framework and the organic template, causing an increase of the diffraction intensities; and ii), a possible reorganization of the siliceous ordered pattern as a consequence of the condensation of free silanol groups, with an increase of the structural order and the consequent increase in the sharpness of the diffraction spots. These two effects are illustrated in the sketches of Fig. 3.

This interpretation of the high temperature data in Fig. 1 and Table 1 is also consistent with the typical cell contraction and intensity increase of the basal peaks, observed during template removal from microporous molecular sieves such as in the case of the silicalite family (25).

TABLE 1 Bragg d-spacings for the three common diffraction spots typical of *T. aurantium* megasleres at 25°C and 250°C and corresponding shifts (Δd)

	d_{100} (nm)	d_{101} (nm)	d_{102} (nm)
25°C	5.14	4.69	3.83
250°C	5.09	4.65	3.80
Δd	0.05	0.04	0.03

TABLE 2 Indices and observed and calculated d-spacings of the 11 spots in the diffraction pattern of *T. aurantium* taken at 250°C

h	k	l	d_{obs} (nm)	d_{cal} (nm)	Δd (nm)
0	0	1	11.4	11.20	−0.20
0	0	2	5.6	5.60	0.00
0	0	3	3.7	3.73	0.03
1	0	0	5.1	5.02	−0.08
1	0	1	4.6	4.58	−0.02
1	0	2	3.8	3.74	−0.06
1	0	3	3.1	3.00	−0.10
1	1	0	2.9	2.90	0.00
1	1	2	2.6	2.57	−0.03
2	0	1	2.5	2.45	−0.05
2	0	2	2.3	2.29	−0.01

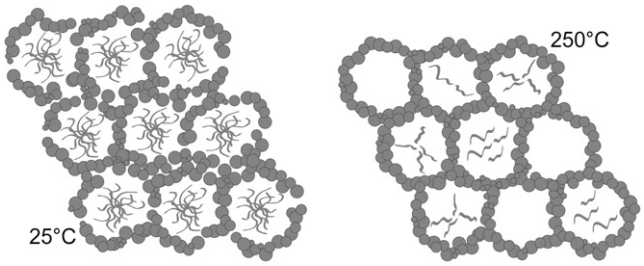

FIGURE 3 Models of the mesoporous arrangements at 25°C and at 250°C. The two sketches show our hypothesis on the ordering evolution of the mesostructure. The small circles, forming a hexagonal pattern, represent the amorphous silica walls and the ribbons schematise the templating protein units.

CONCLUSIONS

The relative dimensions of the thick and hard silica walls and the small central cavity, where the mesostructure with silicatein is located, make sample preparation for electron or scanning microscopy very difficult. So far all our attempts at cutting the samples have completely destroyed the structure. The small angle x-ray diffraction study of siliceous spicules proved to be a very valuable tool to elucidate the organization and disposition of the organic matter inside the amorphous silica envelope. *T. aurantium* strogyloxeas were chosen for this study because their diffraction patterns, especially after thermal treatment, are the richest in diffraction spots. Indeed the appearance of 11 spots in the pattern, recorded after treatment at 250°C, allowed to define unambiguously the presence of a hexagonal lattice and to derive the Miller indices of all the observed spots.

This work triggered us to deepen our study on the structure of spicules and to investigate the quaternary and tertiary structure of silicatein embedded in the mesoporous matrix. As described above, the silicatein protein cannot be extracted from the spicules without strong chemical treatments. Besides, the extracted silicatein appears as a fibrous protein, insoluble in aqueous solvents. These two problems represent an insurmountable obstacle to the study of its three-dimensional structure by NMR or x-ray crystallography. Exploiting the sequence similarity with cathepsin, we then employed the homology modeling method to build a plausible theoretical model of the three-dimensional structure of silicatein (Gianluca Croce, Davide Viterbo, Marco Giovine, and Marco Milanesio, unpublished). From this model we could estimate the volume occupied by a silicatein molecule as 196 nm^3. Therefore each hexagonal cell with volume 282.6 nm^3, obtained from the SAXS data, should contain only one protein molecule. Therefore the templating protein units in each cage are formed by one silicatein molecule possibly surrounded by biological fluid.

The most important outcome of this study of the *T. aurantium* megascleres is the very stringent proof of our hypothesis that nature has organized the organic matter in a single crystal-like hexagonal mesoporous material that can be considered one of the best grown nanostructured composite material so far synthesized or naturally formed.

REFERENCES

1. Garrone, E. 1978. Phylogenesis of Connective Tissue: Morphological Aspects and Biosynthesis of Sponge Intercellular Matrix. S. Karger, Basel, Germany.
2. Shimizu, K., J. Cha, G. D. Stucky, and D. E. Morse. 1998. Silicatein a: Cathepsin L-like protein in sponge biosilica. *Proc. Natl. Acad. Sci. USA.* 95:6234–6238.
3. Cha, J. N., K. Shimizu, Y. Zhou, S. C. Christiansen, B. F. Chmelka, G. D. Stucky, and D. E. Morse. 1999. Silicatein filaments and subunits from a marine sponge direct the polymerization of silica and silicones in vitro. *Proc. Natl. Acad. Sci. USA.* 96:361–365.
4. Voronkov, M. G., G. I. Zelchan, and E. J. Lukevits. 1977. Silicon and Life, 2nd Revised Edition. Zinatne, Riga, Latvia.
5. Perry, C. C., and T. J. Keeling-Tucker. 2000. Biosilicification: the role of the organic matrix in structure control. *Biol. Inorg. Chem.* 5:537–550.
6. Croce, G., A. Frache, M. Milanesio, L. Marchese, M. Causà, D. Viterbo, A. Barbaglia, V. Bolis, G. Bavestrello, C. Cerrano, U. Benatti, M. Pozzolini, M. Giovine, and H. Amenitsch. 2004. Structural characterization of siliceous spicules from marine sponges. *Biophys. J.* 86: 526–534.
7. Croce, G., A. Frache, M. Milanesio, D. Viterbo, G. Bavestrello, U. Benatti, M. Giovine, and H. Amenitsch. 2003. Fiber diffraction study of spicules from marine sponges. *Microsc. Res. Tech.* 62:378–381.
8. De Vos, L., K. Rutzler, and N. Boury-Esnault. 1991. J. Vacelet in Atlas of Sponge Morphology. Smithsonian Institution Press, Washington, DC.
9. Shimizu, K., J. Cha, G. D. Stucky, and D. E. Morse. 1998. Silicatein α: cathepsin L-like protein in sponge biosilica. *Proc. Natl. Acad. Sci. USA.* 95:6234–6238.
10. Amenitsch, H., M. Rappolt, M. Kriechbaum, H. Mio, P. Laggner, and S. Bernstorff. 1998. First performance assessment of the small angle x-ray scattering beamline at ELETTRA. *Synchrotron Radiat.* 5:506–508.
11. Hammersley, A. P. 1995. FIT2D V5.18 Reference Manual V1.6. ESRF Internal Report, EXP/AH/95–01.
12. Hammersley, A. P., S. O. Svensson, M. Hanfland, A. N. Fitch, and D. Häusermann. 1996. Two-dimensional detector software: from real detector to idealised image or two-theta scan. *High Pressure Res.* 14: 235–248.
13. Hunt, J. E., L. Q. Xu, R. E. Winans, and S. Seifert. 2000. Thermal degradation of M41S-class mesoporous sieves as revealed by small-angle x-ray scattering. *Abstracts of Papers of The American Chemical Society.* 219:U681–U681.
14. Barton, T. J., L. M. Bull, W. G. Klemperer, D. A. Loy, B. McEnaney, M. Misono, P. A. Monson, G. Pez, G. W. Scherer, J. C. Vartuli, and O. M. Yaghi. 1999. Tailored porous materials. *Chem. Mater.* 11:2633–2656.
15. Klotz, M., P. A. Albouy, A. Ayral, C. Me´nager, D. Grosso, A. Van der Lee, V. Cabuil, F. Babonneau, and C. Guizard. 2000. The true structure of hexagonal mesophase-templated silica films as revealed by x-ray scattering: effects of thermal treatment and of nanoparticle seeding. *Chem. Mater.* 12:1721–1728.
16. Grosso, D., F. Babonneau, M. Klotz, P. A. Albouy, H. Amenitsch, A. R. Balkenende, A. Brunet-Bruneau, and J. Rivory. 2002. An in situ study of mesostructured CYAB-silica film formation during dip coating using time-resolved SAXS and interferometry measurements. *Chem. Mater.* 14:931–939.
17. Falcaro, P., S. Costacurta, G. Mattei, H. Amenitsch, A. Marcelli, M. Cestelli Guidi, M. Piccinini, A. Nucara, L. Malfatti, T. Kidchob, and P. Innocenzi. 2005. Highly ordered ''defect-free'' self-assembled hybrid films with a tetragonal mesostructure. *J. Am. Chem. Soc.* 127:3838–3846.

18. Garrone, R. 1969. Collagène, spongine et squelette Minéral chez l'éponge Haliclona rosea (O.S.) (Démosponge, Haplosclérides). *J. Microsc.* 8:581–598.

19. Uriz, M. J., X. Turon, and M. A. Becero. 2000. Silica deposition in Demosponges: spiculogenesis in *Crambe crambe*. *Tissue Res.* 301: 299–309.

20. Simpson, T. L., P. F. Langenbruch, and L. Scalera-Liaci. 1985. Silica spicules and axial filaments of the marine sponge *Stelletta grubii* (Porifera, Demospongiae). *Zoomorphology.* 105:375–382.

21. Kresge, C. T., M. E. Leonowicz, W. J. Roth, J. C. Vartuli, and J. S. Beck. 1992. Ordered mesoporous molecular sieves synthesized by a liquid-crystal template mechanism. *Nature*. 359:710–712.

22. Beck, J. S., J. C. Vartuli, W. J. Roth, M. E. Leonowicz, C. T. Kresge, K. D. Schmitt, C. T. W. Chu, D. H. Olson, E. W. Sheppard, S. B. McCullen, J. B. Higgins, and J. L. Schlenkert. 1992. A new family of mesoporous molecular sieves prepared with liquid crystal templates. *J. Am. Chem. Soc.* 114:10834–10843.

23. Zhao, D., Q. Huo, J. Feng, B. F. Chmelka, and G. D. Stucky. 1998. Nonionic triblock and star diblock copolymer and oligomeric surfactant syntheses of highly ordered, hydrothermally stable. *Mesoporous Silica Structures*. *J. Am. Chem. Soc.* 120:6024–6036.

24. Hartmann, M., and A. Vinu. 2002. Mechanical stability and porosity analysis of large-pore SBA-15 mesoporous molecular sieves by mercury porosimetry and organics adsorption. *Langmuir*. 18:8010–8016.

25. Milanesio, M., G. Artioli, A. F. Gualtieri, L. Palin, and C. Lamberti. 2003. Template burning inside TS-1 and Fe-MFI molecular sieves: an in situ XRPD study. *J. Am. Chem. Soc.* 125:14549–14558.